PORE-SCALE MODELLING OF TRANSPORT PROPERTIES IN UNSATURATED CEMENTITIOUS MATERIALS USING LATTICE BOLTZMANN METHOD

M. Zhang

Advanced and Innovative Materials (AIM) Group, Department of Civil, Environmental and Geomatic Engineering, University College London, UK

Abstract

   Transport properties (e.g. permeability and diffusivity) of cementitious materials are usually considered as the main indicators for durability assessment and service life prediction of reinforced concrete structures. In practice, concrete is rarely saturated. Therefore, it is not only of scientific interest but of practical importance to investigate transport properties in unsaturated cementitious materials. This paper presents an integrated modelling scheme to estimate transport properties of cementitious materials with various saturation levels based on their microstructures, which are obtained by X-ray computed microtomography and HYMOSTRUC3D respectively. An in-house code based on single-phase and multiphase lattice Boltzmann models is developed and used to simulate the moisture distribution, permeability and ionic diffusivity of hydrating cement paste. Afterwards, the effects of moisture content and microstructure of cement paste on permeability and ionic diffusivity are investigated in a quantitative manner. The results indicate that the moisture distribution, permeability and ionic diffusivity in unsaturated cement pastes significantly depend on the 3D microstructure. The simulated results show a good agreement with experimental data implying that the proposed modelling scheme provides an effective tool to predict the transport properties in unsaturated cementitious materials.

1.   INTRODUCTION

   Concrete is used in the construction of a wide range of structures. During service, concrete may interact with its environment. For instance, the aggressive chemical species (e.g. chloride, sulphates, carbon dioxide, etc.) from the environment can penetrate into the concrete, thereby leading to a series of degradation processes of the concrete itself or the reinforcement embedded in the structures. These degradation processes strongly relate to the transport phenomena in concrete and transport properties of concrete, e.g. permeability and diffusivity, are usually considered as indicators to evaluate the durability and predict the service life of reinforced concrete structures. In practice, concrete is rarely in a state of full saturation during construction and throughout its long lifetimes due to self-desiccation and wetting-drying cycles. In addition, the corrosion of reinforcing steel in concrete occurs only in an unsaturated state, whereby the oxygen can get access to the rebar surface. Therefore, it is vital to estimate transport properties of partially saturated cementitious materials in order to make an accurate prediction of service life and assessment of durability of reinforced concrete structures.

   In recent years, an increasing attention has been paid to transport properties in unsaturated cementitious materials. Although many efforts including experimental and modelling work have been conducted to qualitatively or quantitatively investigate the effect of moisture

content on transport properties (See [1] for a critical review of these existing efforts), to what extent does the water saturation influence transport properties is still not clear as results published so far show a great dispersion. This can be ascribed to the complexity of microstructure of cementitious materials and simulation of the interaction between liquid/gas and solid in cementitious materials. The main purpose of this study is to quantitatively investigate the effect of degree of water saturation on transport properties in cementitious materials taking into account the 3D microstructure.

2.   3D MICROSTRUCTURE OF CEMENT PASTE

To demonstrate the feasibility of the proposed modelling scheme, the 3D microstructures of cement paste obtained from X-ray computed microtomography (XCT) scans and simulated by the HYMOSTRUC3D model [2] were used in this work, respectively, which are introduced in detail below.

2.1   X-ray computed microtomography

For XCT tests, ASTM type I Portland cement was used. The w/c ratio of the cement paste was 0.5 (mass ratio). After drill mixing in a plastic beaker, small parts of the paste were poured into the syringe and then injected into a micro plastic tube with an internal diameter of 250 µm. The specimen was stored in the standard curing room with a relative humidity of 95% and temperature of 20 ºC and scanned at 1, 7 and 28 days. More details about the XCT testing can be found in [3]. Figure 1a shows the XCT grayscale image of a cylindrical region of interest (ROI) of 7-day cement paste with 200 µm in diameter and 100 µm in thickness extracted from the centre of the reconstructed 3D images, where the cement paste is considered to be most homogeneous. The phases in dark, white and grey represent capillary pore, anhydrous cement grains and hydration products, respectively. In order to identify these three phases in cement phase and quantify the microstructural information, a series of image processing and analysis are required, the details of which were given in [4]. The segmented capillary pore of 7-day cement paste corresponding to the original image in Figure 1a is shown in Figure 1b. For following simulations, a cubic volume of interest (VOI) of $100 \times 100 \times 100$ µm^3 is extracted from the centre of ROI, as shown in Figure 1c.
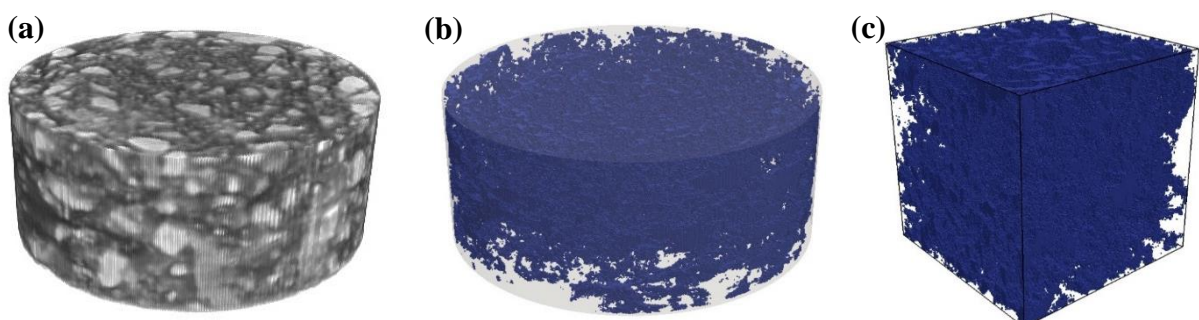

(a)   **(b)**   **(c)**

Figure 1: XCT image and pore structure of 7-day old cement paste: a) XCT grayscale image; b) Pore structure of ROI; and c) Pore structure of VOI

2.2   HYMOSTRUC3D

The simulated 3D microstructure of hardened cement paste by HYMOSTRUC3D was modelled as a composite consisting of pores, anhydrous cement grains and hydration

products, i.e. inner and outer hydration products. An example of the simulated microstructure with size of $100\times100\times100$ μm^3 and the extracted pore structure of cement paste with w/c 0.5 at the age of 28 days is shown in Figure 2. The cement used in the simulation was Portland cement CEM I 42.5 N. A continuous particle size distribution (PSD) with the minimum size of 1 μm and the maximum size of 50 μm was used. The curing temperature was 20 ºC. The simulated microstructure was subsequently digitized into a three-dimensional array of voxels with a resolution of 0.5 μm/voxel that was not only suitable for the solution accuracy but satisfied the computational efficiency [5]. The voxels were assigned to be capillary pore or anhydrous cement or hydration product depending on their corresponding positions.
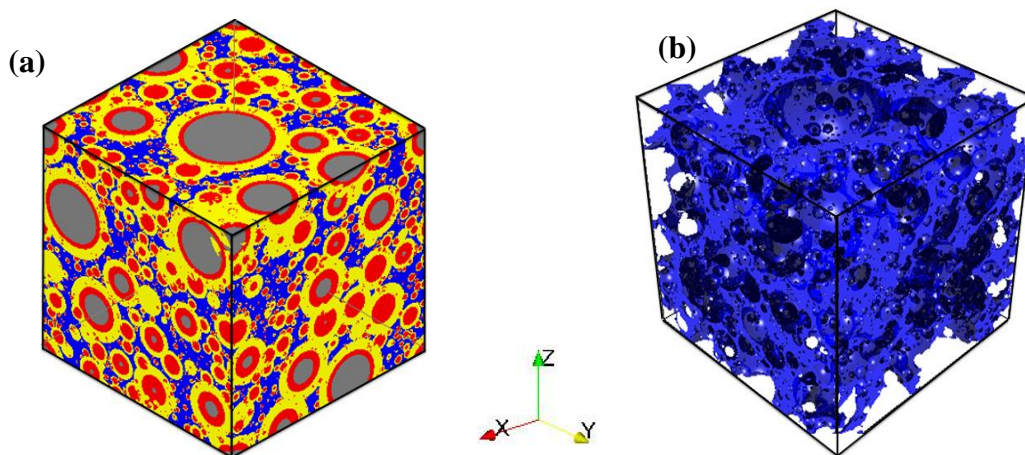

Figure 2: Simulated hardened cement paste with size of $100\times100\times100$ μm^3 by the HYMOSTRUC3D model (w/c = 0.5, t = 28 days): (a) Microstructure; (b) Its pore structure

3. MICROSTRUCTURE-BASED MODELLING AND SIMULATION

The entire modelling procedure for transport properties in unsaturated cement paste consists of the following four main steps.

Step I: Mapping of 3D microstructure onto a discrete cubic lattice with a 1-to-1 correlation of voxel-to-node. The pore voxels are considered as fluid nodes. The solid voxels composed of hydration products and anhydrous cement grains are regarded as impermeable solid nodes.

Step II: Modelling equilibrium distribution of moisture in cement paste with various degrees of water saturation using multiphase lattice Boltzmann method (LBM). The fluid nodes in the cubic lattice are initially saturated with a random homogeneous mixture of water and gas phases with a specific volume ratio corresponding to a given degree of water saturation, S_w. An example of the initial random distribution of moisture at S_w = 50% and S_w = 72% in pore structure of 7-day cement paste obtained from XCT is shown in Figure 3. Liquid and gas phases are represented in blue and white, respectively. Afterwards, the interactions between liquid/gas and solid are simulated using multiphase LBM. The reader is referred to [6] for more details about the developed multiphase lattice Boltzmann model.

Step III: Modelling water and gas permeation through cement paste at various moisture levels using single-phase LBM (see [7] for further information) and calculating the corresponding water and gas permeability as a function of degree of water saturation.

Step IV: Modelling ionic diffusivity using lattice Boltzmann (LB) model for diffusion, the details of which can be found in [8].
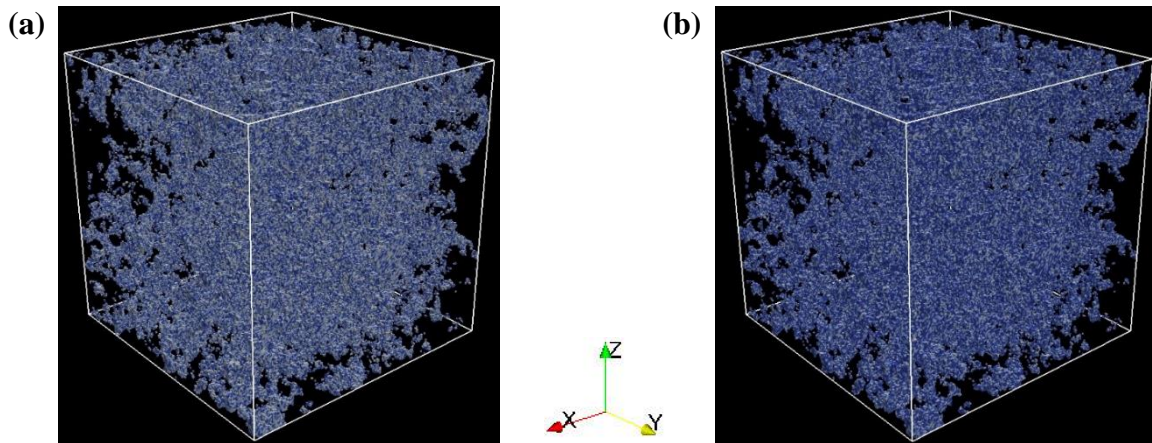
(a)   **(b)**

Figure 3: Initial random distribution of liquid and gas phases in pore structure of 7-day cement paste: (a) $S_w = 50\%$; (b) $S_w = 72\%$. Blue and grey phases represent liquid and gas, respectively

4.   RESULTS AND DISCUSSION

4.1   Moisture distribution

Figure 4 shows the equilibrium distribution of moisture in pore network of 7-day cement paste with water saturation of 50% and 72% respectively corresponding to the initial random distribution of moisture in Figure 3. The equibrium moisture distribution in the microstructure obtained by HYMOSTRUC3D is shown in Figure 5. It can be seen that the liquid covers the solid surface and tends to fill the pores with smaller size, while the gas phase tends to occupy the central region of larger pores and forms many gas phase clusters. The liquid-filled pores provide possible paths for water movement and ion transport. With the obtained equilibrium distribution of moisture in cement paste at various saturation levels, the water/gas permeation and ionic diffusion through unsaturated cement paste can be subsequently simulated following the Steps III and IV, as introduced in Section 3.

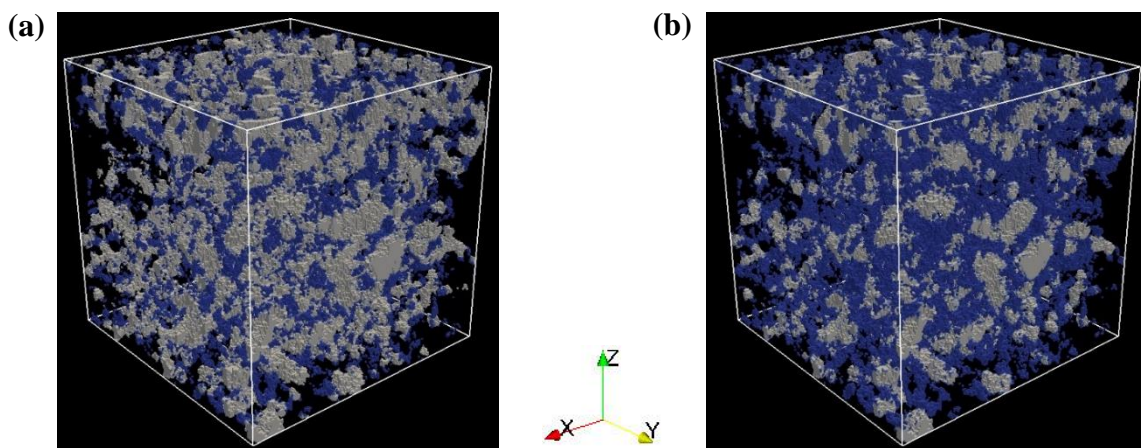**(a)**   **(b)**

Figure 4: Equilibrium distribution of liquid and gas phases in the 7-day cement paste obtained from XCT: (a) $S_w = 50\%$; (b) $S_w = 72\%$. Blue and grey phases represent liquid and gas, respectively
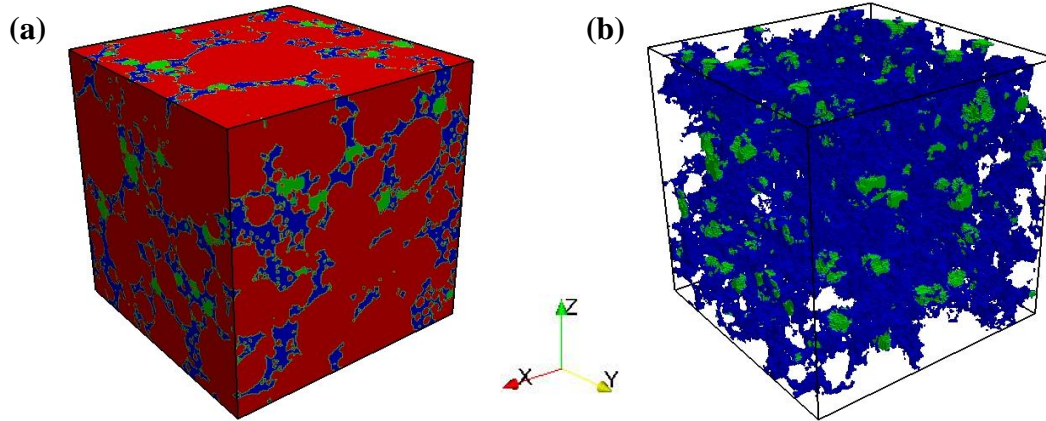
Figure 5: Equilibrium distribution of liquid-gas system with S_w = 83% in the microstructure and pore network of cement paste corresponding to Figure 2. Red, blue and green phases represent solid, liquid and gas, respectively

4.2   Permeability against degree of saturation

Figure 6 shows the steady-state streamline along the flow direction from bottom to top within 7-day cement paste at a water saturation of 72%, the corresponding microstructure and liquid-filled pore network of which can be seen in Figures 1c and 4b. It should be pointed out that in the simulation the gas-filled pores, i.e., 28% of total porosity, are classified into impermeable solid-like nodes and act as obstacles for water permeation. As seen in Figure 6, the water flow is restricted by the impermeable phase composed of anhydrous cement, hydration product and gas, and only passes through the liquid-filled pores. The streamlines have a tortuous configuration and follow the liquid-filled pore network. The flow velocity at some positions (i.e., in dark red) is obviously greater than that in other regions (see Figure 6b). These positions probably correspond to the small liquid-filled pores, which indicates the flow velocity distribution in partially saturated cement paste is highly related to the liquid-filled pore size distribution. It also indicates the LBM used in this study provides insight into the internal velocity distribution at the pore scale and allows one to detect preferential flow paths within the specimen with various degrees of water saturation. Thus, the LB simulation offers a significant potential for new fundamental insights and comprehensive understanding of fluid flow processes in cementitious materials over the whole range of saturation.

The relative water permeability defined as the ratio of the intrinsic water permeability at a certain S_w to that in a fully saturated condition (S_w = 100%), is used to estimate the effect of water saturation. Figure 7a shows the relative water permeability of cement paste as a function of water saturation. For cement paste with various curing ages, there is a significant drop in relative water permeability when the water saturation decreases from 100% to 70% followed by a less dramatic variation until the critical water saturation at which there is no connected liquid-filled pore network allowing water to pass through and the water permeability goes to zero. The dependence of relative water permeability on water saturation for cement paste at different curing ages is slightly different, which can be ascribed to the different microstructure, particularly pore structure, of cement paste at different curing ages. The relative water permeability of 28-day cement paste is more sensitive to a change in water saturation than that of cement paste at 1 and 7 days of curing, as 28-day cement paste has a lower porosity and contains denser, less interconnected and more tortuous pore network and

accordingly the connectivity of liquid-filled pores in 28-day cement paste is more significantly affected by water saturation. All these indicate that water permeability of cement paste at various saturation states highly depend on the 3D microstructure of cement paste.

Figure 7b shows the relative gas permeability that is defined as the ratio between the intrinsic gas permeability at a certain S_w and that in a fully dry condition ($S_w = 0\%$) of cement paste at various curing ages as a function of water saturation. The relative gas permeability is highly influenced by water saturation. As the water saturation increases, there is a sharp decrease in the relative gas permeability for cement paste with various curing ages. Compared to cement paste at 1 and 7 days, the decrease in relative gas permeability of 28-day cement paste with increasing water saturation is more noticeable due to its relatively lower porosity, less interconnected and more tortuous gas-filled pore network at each saturation level.

The simulation results in terms of relative water permeability and relative gas permeability against water saturation agree very well with experimental data in literature [9-11].
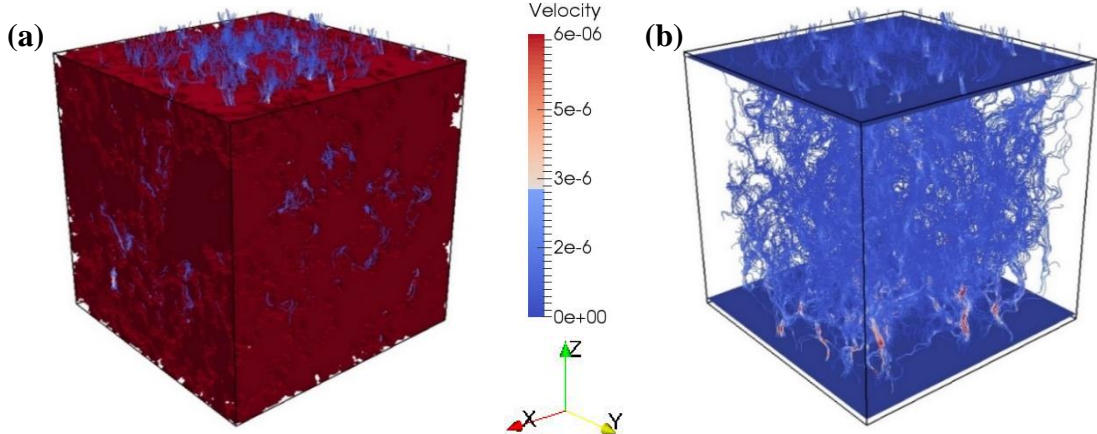

Figure 6: Steady-state water flow in 7-day old cement paste with $S_w = 72\%$: (a) Streamline; (b) Velocity distribution
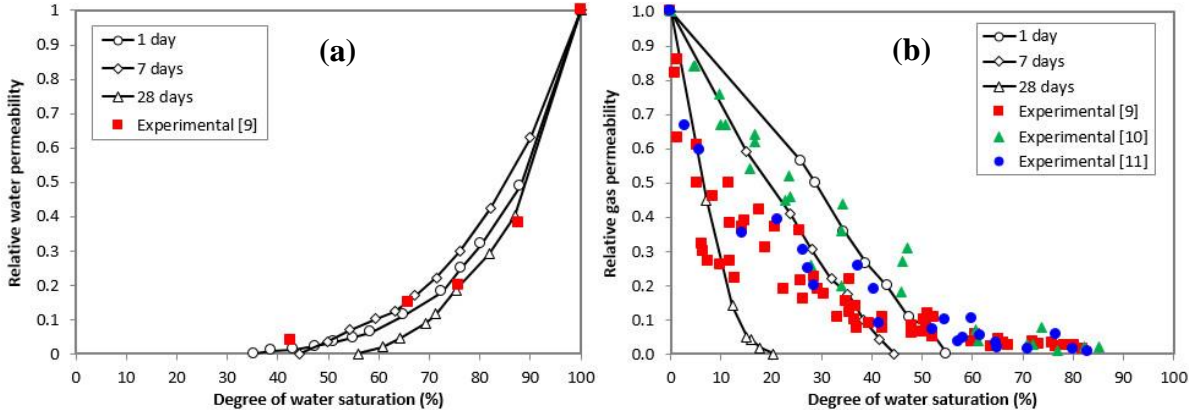

Figure 7: Relative water and gas permeability of cement paste with various curing ages

4.3   Ionic diffusivity against degree of saturation

Figure 8a displays the distribution of ion concentration in the simulated pore structure of cement paste by HYMOSTRUC3D under steady-state condition. It can be seen that the ions only pass through the continuous water way between inlet and outlet. Figure 8b shows the

relative ionic diffusivity as a function of degree of water saturation for 28-day cement paste with w/c ratios of 0.4, 0.5 and 0.6. Obviously, the relative ionic diffusivity shows a strong dependence on the degree of water saturation. For w/c = 0.5, there is a significant decrease in diffusivity when the water saturation degree diminishes from 100% to 47% followed by a less dramatic variation of diffusivity within the range of saturation between 47% and 21.6%. At a saturation of 21.6%, the ionic diffusivity gets to zero because there is no connected path in the liquid-filled pore network allowing the ionic species to pass through. This implies that the critical water saturation for w/c = 0.5 cement paste where depercolation occurs is 21.6%. It can be seen that the simulation results show a similar trend to the literature experimental data [12,13], despite that the sample used in the simulation is cement paste while the specimens tested in literature are mortars. Mortar can be considered to be a cement paste-sand composite where sand is relatively impermeable as compared to cement paste and the ionic diffusivity in mortar is dominated by capillary pores in cement paste.
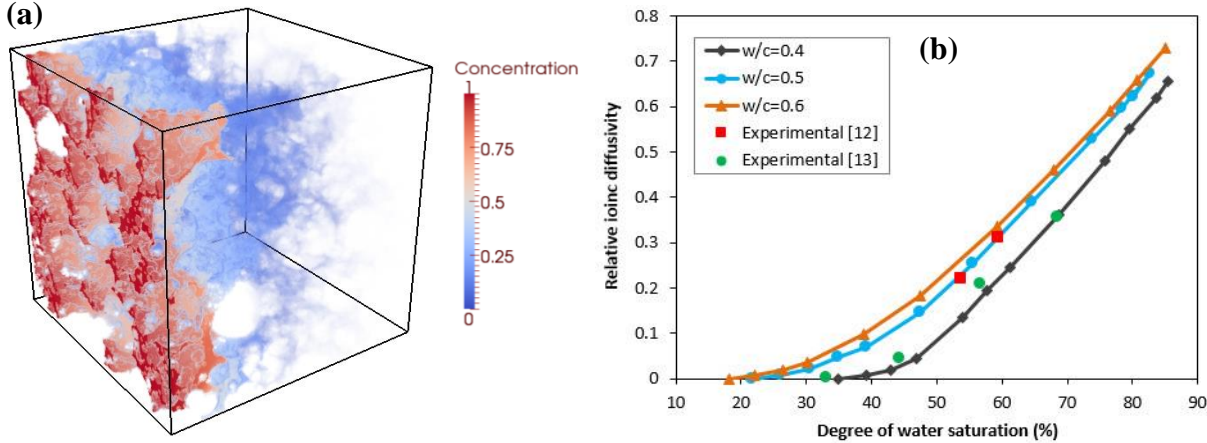

Figure 8: Distribution of steady-state ion concentration and relative ionic diffusivity of simulated cement paste (w/c = 0.5, t = 28 days) by HYMOSTRUC3D

5.   CONCLUSIONS

−   At a certain degree of water saturation, the liquid phase covers the surface of solid phase and tends to fill the pores with smaller size, while the gas phase tends to occupy the central region of larger pores and forms many gas phase clusters. In addition, the distribution of liquid and gas in unsaturated cementitious materials depends not only on pore size but also on solid phase in terms of shape, size, connectivity and tortuosity, which are all included in the 3D microstructure of cementitious materials.

−   There exists a critical water saturation at which the liquid-filled or gas-filled capillary porosity becomes disconnected. The critical water saturation is highly associated with microstructure. For cement paste with curing ages of 1, 7 and 28 days obtained from XCT, the critical water saturations are found to be 35%, 41% and 56%, respectively, while the critical water saturation for ionic diffusivity of w/c = 0.5 cement paste with curing age of 28 days generated from HYMOSTRUC3D is 21.6%.

−   The degree of water saturation has a significant influence on both permeability and ioinc diffusivity of cement paste with various. curing ages. As degree of water saturation decreases, there is a gradual drop in water/gas permeability and ioic diffusivity followed

by a sharp decrease when the water saturation level is approaching the critical water saturation.

– The simulated water/gas permeability and ionic diffusivity of cementitious materials as a function of water saturation show good agreement with experimental data in literature.

ACKNOWLEDGEMENTS

REFERENCES

[1] Zhang, Y., Zhang, M. and Ye, G., 'Transport properties in unsaturated cement-based materials – A review', *Constr. Build. Mater.* **72** (2014) 367-379.

[2] van Breugel, K., 'Simulation of hydration and formation of structure in hardening cement-based materials', PhD thesis, Delft University of Technology, Delft, 1991.

[3] Zhang, M., He, Y., Ye, G., Lange, D.A. and van Breugel, K., 'Computational investigation on mass diffusivity in Portland cement paste based on X-ray computed microtomography (μCT) image', *Constr. Build. Mater.* **27** (1) (2012) 472-481.

[4] Zhang, M. and Jivkov, A.P., 'Micromechanical modelling of deformation and fracture of hydrating cement paste using X-ray computed tomography characterisation', *Compos. Part B Eng.* **88** (2016) 64-72.

[5] Zhang, M., Ye, G. and van Breugel, K., 'A numerical-statistical approach to determining the representative elementary volume (REV) of cement paste for measuring diffusivity', *Mater. Construcc.* **60** (300) (2010) 7-20.

[6] Zhang, M., Xu, K., He, Y. and Jivkov, A.P., 'Pore-scale modelling of 3D moisture distribution and critical saturation in cementitious materials', *Constr. Build. Mater.* **64** (2014) 222-230.

[7] Zhang, M., Ye, G. and van Breugel, K., 'Microstructure-based modeling of permeability of cementitious materials using multiple-relaxation-time lattice Boltzmann method', *Comp. Mater. Sci.* **68** (2013) 142-151.

[8] Zhang, M., Ye, G. and van Breugel, K., 'Modeling of ionic diffusivity in non-saturated cement-based materials using lattice Boltzmann method, *Cem. Concr. Res.* **42** (11) (2012) 1524-1533.

[9] Zamani, S., Kowalczyk, R.M. and McDonald, P.J., 'The relative humidity dependence of the permeability of cement paste measured using GARField NMR profiling', *Cem. Concr. Res.* **57** (2014) 88-94.

[10] Kameche, Z.A., Ghomari, F., Choinska, M. and Khelidj, A., 'Assessment of liquid water and gas permeabilities of partially saturated ordinary concrete', *Constr. Build. Mater.* **65** (2014) 551-565.

[11] Wardeh, G. and Perrin, B., 'Relative permeabilities of cement-based materials: influence of the tortuosity function', *J. Build. Phys.* **30** (2006) 39-57.

[12] Nielsen, E.P. and Geiker, M.R., 'Chloride diffusion in partially saturated cementitious material', *Cem. Concr. Res.* **33** (2003) 133-138.

[13] de Vera, G., Climent, M.A., Viqueira, E., Anton, C. and Andrade, C., 'A test method for measuring chloride diffusion coefficients through non-saturated concrete. Part II: the instantaneous plane source diffusion case with chloride binding consideration', *Cem. Concr. Res.* **37** (2007) 1113-1123.